5-2021

Guide RNAs preparation for in-vitro CRISPR-Cas9 complex delivery targeting genes that affect wound healing.

Prashant Khatiwada

Guide RNAs preparation for in-vitro CRISPR-Cas9 complex delivery targeting genes that affect wound healing.

Honors Thesis by Prashant Khatiwada

Department of Biomedical Engineering

College of Engineering

University of Arkansas

Fayetteville, AR 72701

Faculty Mentor: Dr. Christopher Nelson

Honors Coordinator: Dr. Kyle Quinn

Table of Contents

1. Abstract

CRISPR-Cas9 technology has widely been used as a viable genome engineering platform to make site-specific insertion, deletion, and breaks. The nuclease dead version of Cas9 or dCas9 can be used for the activation and repression of target gene sites using specific activation or repression domains. In this study, CRISPR guide RNAs were designed for a CRISPR inhibition approach to repress the transcriptional activity of the target genes. An expression plasmid vector composed of a U6 promoter sequence, BbsI restriction sites, and a chimeric gRNA sequence was digested, and the phosphorylated forward and reverse gRNAs were ligated with the plasmid vector. The expression plasmids were transformed in *E.coli* cells and plated on Agar plates for selective extraction of the expression plasmids with the desired gRNA sequence from the bacterial cells. The presence of gRNAs was confirmed in the expression vectors through Sanger sequencing, and the cloned gRNAs in the expression vectors were transfected into HEK293 cells along with dCas9-KRAB through a lipid-mediated delivery method. The gRNAs were designed for NF-κB, NFKBIZ, and Caveolin-1 genes, among which the gRNAs for NF-κB were transfected to the HEK293 cells. The target genes were chosen because of their upregulated expression at impaired wound healing conditions. NF-κB is associated with several physiological pathways, gene expression, and protein functions involved in wound healing. The upregulation of NF-κB is associated with the negative proliferative phase, extended inflammatory response, and altered phagocytic functions of macrophages (Khanna et al., 2010). An increased expression of NFKBIZ is linked with the upregulation of IL-6 gene expression causing extended inflammation (Trinh et al., 2008), (Johnson et al., 2020). Over expression of Cav1 is known to affect the movement of keratinocytes and epithelial cells, affecting wound closure (Jozic et al., 2019).

2. Introduction

2.1 CRISPR/Cas9

Clustered Regularly Interspaced Palindromic Repeats or CRISPR technology has introduced a new chapter in the world of genome engineering through its use with respective CRISPR-associated protein (Cas) nucleases. Originating from the type II CRISPR-Cas systems, CRISPR with Cas9 endonuclease uses a ribonucleic acid duplex to make double-strand breaks at specific targets in the DNA (Doudna & Charpentier, 2014). CRISPR-Cas9 can be used with a specific DNA target with an engineered single-guide RNA (sgRNA) upstream of a protospacer adjacent motif (PAM) sequence to make site-specific DNA cleavages. The sgRNA incorporates CRISPR RNA (crRNA) and trans-activating RNA (tracrRNA) such that the 5' end of the sequence uses nucleotide base pair binding with a specific DNA site and double-stranded RNA complex at the 3' end binds with the Cas9 (Jinek et al., 2012).

2.2 dCas9- KRAB

The nuclease-dead version of the Cas9 can be used for genome regulation, where a mutant Cas9 changes the regulation of the transcription of the genes and does not contribute to gene editing. Also called CRISPR interference or CRISPRi, dCas9 can be used as a gene silencing method by blocking the transcription of the genes. Using domains such as Krüppel-associated box (KRAB) with dCas9 helps in the repression of transcription in mammalian cells including human cells (Gilbert et al., 2013). Similarly, gene expression can be activated using activator domains like VP64 with dCas9, which is also called CRISPR activation (CRISPRa). Unlike Cas9 that makes a double-stranded

break in the target sequence through RuvC and HNH nuclease domains, dCas9 consists of the deactivated nuclease domains caused by the introduced mutations of the two nuclease domains. The nuclease dead Cas9 functions as a protein that binds with DNA and is guided by an RNA sequence. Thus, effectors like VP64 and KRAB induce an artificial transcription factor when combined with sgRNA (La Russa & Qi, 2015).

2.3 Lipid Transfection

Lipid transfection uses a lipid complex that resembles the cell membrane's phospholipid bilayer to deliver nucleic acids through the cell membrane into the cytoplasm and ultimately to the nucleus. Because lipids are fat-soluble molecules, lipid-mediated transfection uses small lipid vesicles to travel through bi-layer cell membranes which are hydrophilic towards the cytoplasm and extracellular matrix, and hydrophobic in between (Carter & Shieh, 2015). Lipofectamine Reagent, also considered as the "gold standard" for the efficient transfection of nucleic acids, can surpass the metabolic degradation during the delivery into the cells (Cardarelli et al., 2016).

2.4 Guide RNA

To design guide RNA for genome engineering applications, there are certain design criteria to be considered. Depending on the type of Cas9 nucleases and CRISPR approaches, the target region may differ with respect to the PAM sequence. In *Streptococcus pyogenes* Cas9 (SpCas9), for a CRISPRa approach, an ideal gRNA is considered to have a ~100 nucleotides window upstream of the Transcription Start Site (TSS) of the gene whereas, for a CRISPRi approach, a region with a ~100 nucleotides

window downstream to the TSS is considered ideal (Mohr et al., 2016). Guide RNAs with mismatches away from the PAM are more favorable than the guides whose mismatches are closer to the PAM. (Addgene, n.d.). The favorable GC content on the gRNA sequence varies based on the applications in different cell lines. In mammalian cells, a GC percentage of 40% to 60 % is considered favorable. The guide sequence is generally 17-20 nucleotides long and is complementary to the target DNA. The PAM sequence for SpCas9 is 3 nucleotides long- NGG, where "N" can be a variable nucleotide of the target DNA. If the gRNAs are inserted with the U6 Promoter, a "G" nucleotide is preferred at the beginning of each guide sequence for the initiation of transcription (Schindele et al., 2020).

Using a specific restriction endonuclease, specific cuts can be made at the target DNA sites on a plasmid vector for a "classic cloning" approach. Using overhangs that are complementary to both the gRNA and the plasmid vector, the blunt ends can be joined using a ligation reaction, where a T4 DNA Ligase catalyzes the joining process of the complementary regions. Similarly, there are a number of cloning methods such as the Gateway® Recombination Cloning, Gibson Assembly, Golden Gate, Molecular Cloning, etc. which can be used for the insertion of desired gRNA sequences into the plasmid DNAs. (Addgene, n.d.).

2.5 Nuclear Factor-Kappa Light Chain Gene Enhancer of Activated B cells:

Nuclear Factor-κB or NF-κB is a transcription factor that activates various genes that are associated with cytokines, molecules for leukocyte adhesion, chemokines, and the survival of cells. NF-κB has an essential role behind the vascular complications and

dysfunction in diabetes among which the upregulated expression of tumor necrosis factor-α (TNF-α), transforming growth factor-β (TGF-β), B-cell lymphoma 2 (BcL2), and other pro-apoptotic genes trigger vascular dysfunction. (Collins & Cybulsky, 2001). Likewise, with activated NF-κB, the receptor for advanced glycation end-products (RAGE) experiences an increased expression along with other proinflammatory cytokines which promote the signaling for cell damage (Tobon-Velasco et al., 2014). Advanced glycation end products (AGEs) that bind with RAGE, and reactive oxygen species (ROS) are induced by Hyperglycemia and increased pro-inflammatory response through NF-κB activation (LV et al., 2016). Overproduction of NF-κB also leads to angiogenesis along with cell damage as it affects the gene expression of endogenous protective factors, vascular endothelial growth factor (VEGF), platelet-derived growth factor (PDGF), and endothelin-1 (ET-1) (Kitada et al., 2010). Since the cell signaling molecules for NF-κB are activated because of hyperglycemia, primarily through the AGE pathway, the altered gene expression as well as protein functions can lead to irregularities in inflammation, blood flow, leukocyte adhesion, membrane permeability, and apoptosis (Rask-Madsen & King, 2010).

The upregulation of NF-κB is indicative of negative physiological effects, wound healing, and other cellular functions in hyperglycemic/ diabetic conditions. While several growth factors, pathways, and genes are activated along with NF-κB, the regulation of NF-κB is controlled by its inhibitors. NF-κB has an amino acid domain, also known as the Rel homology domain, which is associated with NF-κB inhibitors or IκBs. The inhibitors keep the NF-κB dimers from entering the nuclear region and the dimers remain in the cytoplasmic region. With the phosphorylation and activation of IKK kinase complex,

consisting of heterodimers such as IKK-α, IKK-β, and IKK-γ subunits, the NF-κB inhibitors or IκBs are phosphorylated as well. The inhibitors are then polyubiquitinated and eventually degraded which triggers the movement of NF-κB from the cytoplasm to the nucleus (Collins & Cybulsky, 2001).

NF-κB is associated with wound healing physiological processes, especially in diabetic conditions, because of its relationship with other growth factors. For instance, the increased levels of TNF-α cytokines are found in the macrophages of diabetic mice wounds, which indicates an extended inflammatory response. The defective phagocytic functions of macrophages derived from altered VEGF in diabetic animal models negatively affect the extracellular matrix deposition, therefore affecting the proliferative phase of wound healing and tissue repair (Khanna et al., 2010).

2.6 Nuclear Factor of Kappa Light Polypeptide Gene Enhancer in B-Cells Inhibitor Zeta

NFKBIZ is a single copy gene and codes for the IκBζ protein. The IκBζ protein binds with NF-κB p50 homodimers unlike other IκB proteins, and increases the expression of the IL-6 gene (Trinh et al., 2008). The expression of IL-6 is found to be upregulated in diabetic wound sites, therefore, resulting in inflammation that lasts longer and delayed wound healing (Johnson et al., 2020). Additionally, patients with Type 2 diabetes have an upregulated gene expression for NFKBIZ (Takematsu et al., 2020).

2.7 Caveolin-1

Caveolin-1 or Cav1 is found upregulated in the biopsies of non-healing diabetic foot ulcers whereas they are downregulated in the healing wounds. Cav1 is associated with membranous glucocorticoid receptors (mbGRs) as well as epidermal growth factor receptors (EGFR) to interfere with the migration of keratinocytes and epithelial cells for wound closure. The knockdown of Cav1 using CRISPR/Cas9 indicated a regulated wound healing and epithelialization by negatively affecting the complexes of Cav1-mbGR and Cav1-EGFR (Jozic et al., 2019). For diabetes-induced oxidative stress on in vivo wounds and in vitro dermal fibroblasts, an upregulated Cav1 expression isolated Mdm2 away from p53 which negatively affected the fibroblasts from type-2 diabetic patients. The down-regulated expression of Cav1 at specific targets enhanced tissue repair and indicated the crucial role of Cav1 in delayed wound healing in diabetes as well as high oxidative stress causing cellular senescence (Bitar et al., 2013).

Cav1 binds with a widely distributed glycoprotein CD26 and regulates T-cell proliferation. When interacting proteins Tollip and IRAK-1 dissociate from Cav1, it upregulates CD86 through the activation of NF-κB (Ohnuma et al., 2005).

NF-κB has associations with several genes, signaling pathways, growth factors, and proteins including NFKBIZ and Caveolin-1, which are involved in wound-healing processes.

3. Materials and Methods

3.1 Guide RNA design

The guide RNAs for NF-kB were designed and selected using online platforms: CRISPR RGEN Tools (rgenome, n.d.), NCBI-BLAST (NCBI, n.d.), UCSC Genome Browser (UCSC, n.d.). The forward and reverse primers were designed to align with the following nucleotide sequence:

5'- CACC NNNNNNNNNNNNNNNNNNN 3'

3'- NNNNNNNNNNNNNNNNNNNN CAAA- 5'

Where, CACC and CAAA at the 5' regions were the sticky regions for the complementary forward and reverse primers respectively, and the "N" represented the guide RNA sequence nucleotides.

The gRNA sequences for NF-kB in spCas9

NF-kB: Forward Oligo	NF-kB: Reverse Oligo
1. GGGGAAGCCCGCACTTCTAG	1. CTAGAAGTGCGGGCTTCCCC
2. GGGGGAAGCCCGCACTTCTA	2. TAGAAGTGCGGGCTTCCCCC
3. GTGGGGGAAGCCCGCACTTCT	3. AGAAGTGCGGGCTTCCCCCAC
4. GCGAGAGAGCATACAGACAGA	4. TCTGTCTGTATGCTCTCTCGC
5. GTATGCTCTCTCGACGTCAG	5. CTGACGTCGAGAGAGCATAC

Table 1.: The forward gRNA oligos listed with their respective reverse gRNA oligos for NF-kB

The gRNA sequences for NFKIZ in spCas9

NFKBIZ: Forward Oligo	NFKBIZ: Reverse Oligo
1. GGGACGGCGCGGGCCAGTAC	1. GTACTGGCCCGCGCCGTCCC
2. GGCGCGCCCCGAGTACGCAG	2. CTGCGTACTCGGGGCGCGCC
3. GCTGCGCGCGGCTGCCTCCC	3. GGGAGGCAGCCGCGCGCAGC

Table 2: The forward gRNA oligos listed with their respective reverse gRNA oligos for NFKBIZ

The gRNA sequences for Cav1 in spCas9

Cav1: Forward Oligo	Cav1: Reverse Oligo
1. GGGAGCCGTAGCTGTCGGAG	1. CTCCGACAGCTACGGCTCCC
2. GCTAACCGCTCCGACAGCTA	2. TAGCTGTCGGAGCGGTTAGC
3. GTGAGAAGTCAGCCTGGCGG	3. CCGCCAGGCTGACTTCTCAC

Table 3: The forward gRNA oligos listed with their respective reverse gRNA oligos for Cav1

In this study, of the designed gRNAs for NF-κB, NFKBIZ, and Cav1, only the gRNAs for NF-κB were transfected in the cells for further analysis.

3.2 Oligos/ gRNA Stock

Each tube containing either the forward or the reverse guide RNA sequence was re-suspended with an appropriate amount of nuclease-free water to get final concentrations of 100 µM. The re-suspended oligos were stored at -20°C.

3.3 Plasmid Digestion

For the digestion of plasmid DNA containing U6 promoter sequence, chimeric gRNA sequence, BBsI restriction sites, the restriction enzyme BbsI was used. 1.13 µL of plasmid DNA was mixed with 2 µL of the restriction enzyme along with 10 µL of 10X cut buffer and 86.87 µL of sterile molecular bio water to get a plasmid stock of 100 µL. The plasmid stock was incubated at 37 °C for an hour to get a digested plasmid stock. The plasmid was run in an agarose gel electrophoresis to confirm the digestion of plasmids.

3.4 Phosphorylation of Primers

For each guide RNA, 8.5 µL of the oligo stock containing the forward guide RNA sequence, and 8.5 µL of the oligo stock containing the reverse guide RNA sequence were mixed along with 2 µL of T4 DNA Ligase Buffer, 1µL of T4 Polynucleotide Kinase (PNK), and 0.5 µL of Adenosine Triphosphate (ATP) in PCR tube strips. In a PCR block, the tube strips were run at 37 °C for 60 minutes, 65 °C for 20 minutes, 95 °C for 2 minutes, cooled to RT for 25 minutes and the temperature was dropped to 4°C before the guide RNAs were ligated with the plasmids.

3.5 Ligation

2 µL of digested plasmid was mixed with 1µL of phosphorylated oligos or insert along with 2 µL of T4 DNA Ligase Buffer, 1 µL of T4 Ligase and 14 µL of water. The final mixture with the volume of 20 µL was incubated at 16 °C in a PCR block for at least 2 hours.

3.6 Transformation

STBL3 *E. coli* cells stored in -80ºC were thawed in ice before mixing 50 µL of the *E. coli* cells with 2.5 µL of the ligated plasmid DNA. For transformation of the plasmids in the cells, they were incubated on ice for 30 minutes, heat-shocked for a minute at 42ºC temperature, and placed on ice for 2 minutes. The plasmids-cells were mixed with 250 µL of Super Optimal Growth (SOC) media and incubated on a shaker at 37 º C temperature for 60 minutes. After incubation, they were plated on agar plates treated with Carbenicillin antibiotic and placed in an incubator overnight maintained at 37ºC.

Once the plates had visible colonies, a colony for each gRNA/ plasmid was collected and inoculated into 5 ml of LB Broth media and placed in a shaker at 37º C for 16 hours. For selective transformation of the plasmids of interest, 5 µL of Carbenicillin was added for a 1:1000 antibiotic dilution.

After 16 hours, the LB Broth with cells were centrifuged at 4000 rpm for 15 minutes. The supernatant was discarded, and the pellet was used to extract the plasmid DNA using the QIAprep Spin Miniprep Kit (QIAGEN, n.d.). The extracted plasmids were sequenced through the Sanger sequencing services from Eurofins Genomics LLC. (Eurofins Genomics, n.d.).

3.7 Cell Culture

Frozen HEK293 cells were thawed in a water bath at 37°C and mixed with DMEM medium containing 100 units/ml of penicillin G sodium, 100 µg/ml of streptomycin, 4 mM of L-glutamine, 10% of fetal bovine serum. The media with the cells was centrifuged for 10 minutes, the supernatant was discarded, and the pellet obtained was resuspended with DMEM medium. The cells were transferred to a tissue culture flask and incubated at 37°C. The cells were passaged when they reached 70-80% confluency. For passaging the cells, the medium was aspirated and washed with 10 ml PBS. 5 ml of Trypsin-EDTA was added to the flask, incubated for 5 minutes and the growth medium was added to inhibit the function of Trypsin. The cells were diluted with Trypan Blue solution and counted in a hemocytometer before seeding around 180,000 cells along with 1 mL media in each well in a 12-well plate. The 12-well plate was incubated for 24 hours at 37°C.

3.8 Transfection

To transfect the cells in a 12-well plate, two microcentrifuge tubes were prepared for each well. 500 ng of dCas9-KRAB plasmid and 500 ng of the primers with gRNA were diluted in Opti-MEM™ Medium, and P3000™ Reagent in the first microcentrifuge tube and Lipofectamine™ 3000 Reagent was diluted in Opti-MEM™Medium in the second microcentrifuge tube. The contents of the two microcentrifuges were mixed by transferring the contents of the first tube to the second tube in a 1:1 ratio. The final mixture in each tube was transferred to the respective wells containing the cells using a micropipette while also gently rocking the 12-well plate in the process.

Wells A1 and A2 were added with the mixture (1:1 ratio) of 500 ng GFP-plasmid diluted in Opti-MEM™ Medium, and Lipofectamine™ 3000 Reagent diluted in Opti-MEM™Medium (Thermofisher, n.d.). Wells A1 and A2 served as the positive controls and the well A4 contained only the cell culture media to serve as a negative control**.** Wells A1, A2 were transfected with plasmids with GFP. Well A3 was transfected with the gRNA (GTGGGGGAAGCCCGCACTTCT) and dCas9-KRAB, well A4 was not transfected and served as the negative control. Wells B1 and C1 were transfected with the gRNA (GGGAAGCCCGCACTTCTAG) along with dCas9-KRAB, wells B2 and C2 were transfected with the gRNA (GGGGGAAGCCCGCACTTCTA) along with dCas9-KRAB, wells A3 and C3 were transfected with the gRNA (GTGGGGGAAGCCCGCACTTCT) along with dCas9-KRAB, and wells B4 and C4 were transfected with the gRNA (GTATGCTCTCTCGACGTCAG) along with dCas9-KRAB in duplicates. After 24 and 48 hours of transfection, the cells in the wells of the 12-well plate were imaged using Nikon Eclipse Ts2 inverted microscope. The positive control cells transfected with GFP were imaged with an Epi-fluorescence imaging setting and the cells transfected with dCas9-KRAB and gRNAs were imaged with a Diascope imaging setting. For the verification of transcriptional repression by dCas9-KRAB proteins in the transfected cells, the RNA extracted from the transfected and cultured cells using RNeasy Mini Kit (QIAGEN, n.d.) would be quantified.

The primers for qPCR were designed and analyzed using online platforms like NCBI Primer-Blast (NBBI, n.d.), Origene (Inc., O.G.T. (n.d.)) and UCSC Genome Browser (UCSC, n.d.).

The designed forward and reverse primers for qPCR: NF-kB

NF-kB: Forward Primer	NF-kB: Reverse Primer
1. 1CTGCCAACAGATGGCCC	1. CACCATGTCCTTGGGTCCAG
2. AAAAGAACCACCAGCTTCAGA	2. GCAGTGCCATCTGTGGTT
3. GTATTTCAACCACAGATGGCAC	3. CGGAAACGAAATCCTCTCTGT

Table 4: The forward qPCR primers listed with their respective reverse qPCR primers for NF-kB

The designed forward and reverse primers for qPCR: NFKBIZ

NFKBIZ: Forward Primer	NFKBIZ: Reverse Primer
1. CCGATTCGTTGTCTGATGGACC	1. GCACTGCTCTCCTGTTTGGGTT
2. TCAGACGGCGAGTTCTTAGAG	2. GAGAGTTCAGCATCAGGCCA
3. ATGCTGTCACGTACTTGGGTTA	3. ATCCACAGCTTGGCCAGAAG

Table 5: The forward qPCR primers listed with their respective reverse qPCR primers for NFKBIZ

The designed forward and reverse primers for qPCR: Cav1

Cav1: Forward Primer	Cav1: Reverse Primer
1. CCAAGGAGATCGACCTGGTCAA	1. GCCGTCAAAACTGTGTGTCCCT
2. CTGGTCAACCGCGACCCTAA	2. CTGGCCTTCCAAATGCCGTC
3. TCGGAGCGGTTAGTTCGATT	3. TAGACACGGCTGATGCACTG

Table 6: The forward qPCR primers listed with their respective reverse qPCR primers for Cav1

4. Results

4.1 Plasmid Digestion Verification

Agarose Gel Electrophoresis

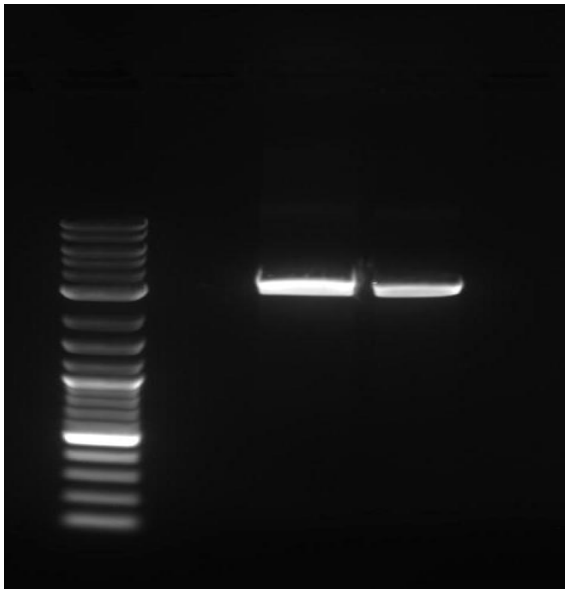

Figure 1: 1% TBE agarose gel showed the presence of single bands on wells 3 and 4, corresponding to ~3.0 kilobases indicating cleaved plasmids.

The appearance of a single band in each of the two wells corresponding to ~3.0 kilobases indicates that the plasmid samples were cleaved by the restriction enzyme BbsI, therefore retaining the 3223 bp or ~3.2 kilobases of the plasmid.

4.2 Sanger Sequencing Verification

Sequence analysis of gRNA- GGGGAAGCCCGCACTTCTAG

(2a)

Sequence analysis of gRNA- GGGGGAAGCCCGCACTTCTA

(2b)

Sequence analysis of gRNA- GTGGGGGAAGCCCGCACTTCT

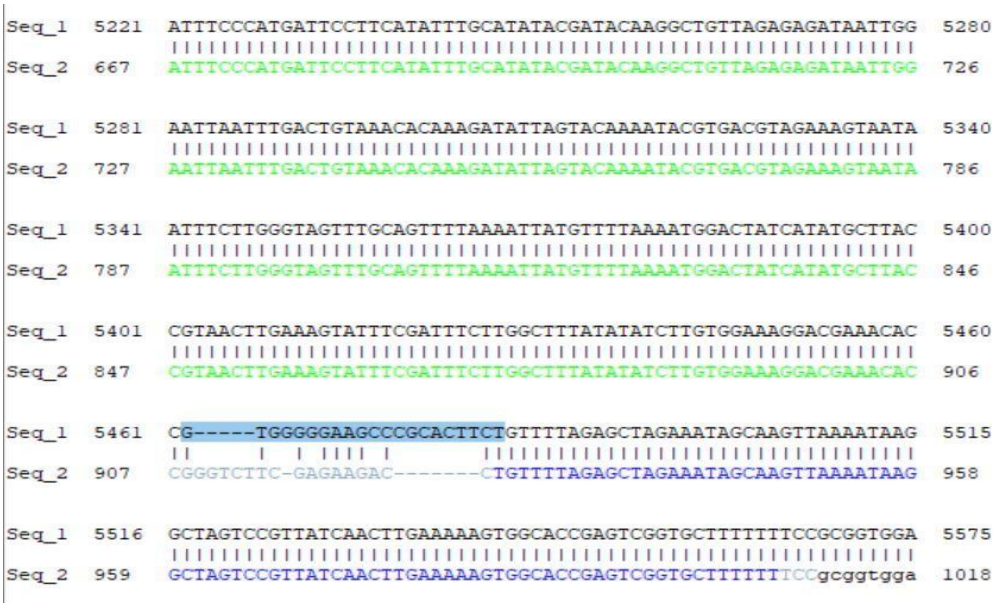

(2c)

Sequence analysis of gRNA- GCGAGAGAGCATACAGACAGA

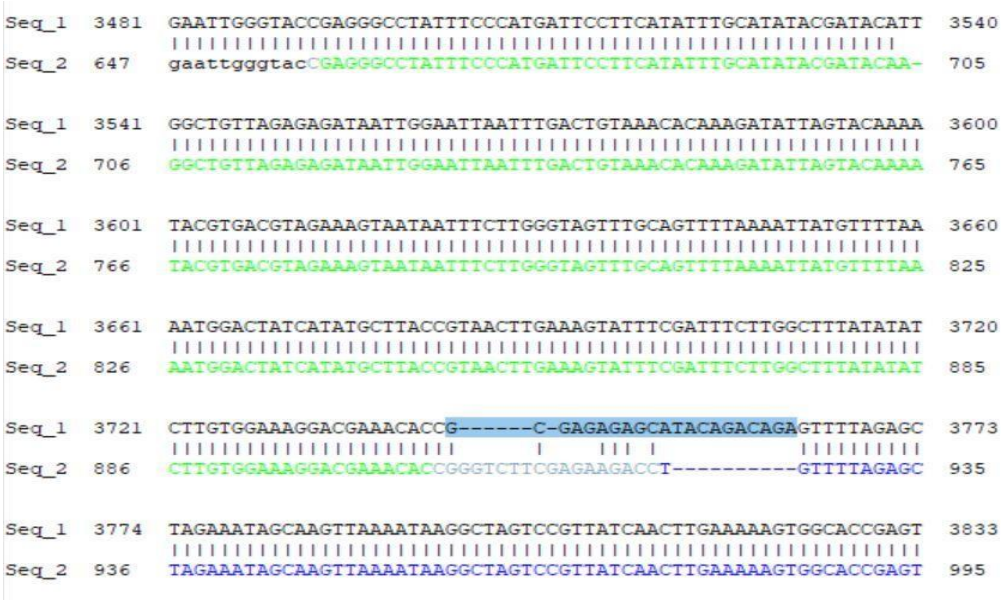

(2d)

Sequence analysis of gRNA- GTATGCTCTCTCGACGTCAG

(2e)

Figures (2a-2e): Alignment of the expression plasmid backbone (Seq_2) with the respective experimental plasmids containing gRNAs for NF-κB (Seq_1). The presence of the forward gRNA inserts (highlighted in Blue in Seq_1) in the experimental vectors between the U6 Promoter sequence (green colored nucleotides) and the tracrRNA sequence (blue colored nucleotides).

The presence of forward gRNA sequences:

1. GGGGAAGCCCGCACTTCTAG
2. GGGGGAAGCCCGCACTTCTA
3. GTGGGGGAAGCCCGCACTTCT
4. GCGAGAGAGCATACAGACAGA
5. GTATGCTCTCTCGACGTCAG

confirms the successful insertion of gRNAs in the plasmid vector used. Based on the Sanger Sequencing results analyzed on "Serial Cloner 2.1", the first gRNA sequence was present from 4102 to 4121 base pairs, the second gRNA sequence was present from 4092 to 4111 base pairs, the third gRNA sequence was present from 5462 to 5482 base pairs, the fourth gRNA sequence was present from 3743 to 3763 base pairs and, and the fifth gRNA sequence was present from 4234 to 4253 base pairs in the experimental plasmid vectors cloned with gRNAS. In figures 2a-2e. "Seq_1" represented the sequence of the plasmid vector with gRNA, and "Seq_2" represented the sequence of the uncleaved plasmid vector. All five gRNA inserts were present in the BBsI sites between the U6 promoter (represented by the green-colored nucleotide bases in Seq_2 of Figure 2a-2e) and the chimeric RNA sequence (represented by the blue colored nucleotide bases in

Seq_2 of Figures 2a-2e). Each gRNA insert corresponded to the BBsI site of the uncut plasmid (~907-924 nt).

The U6 promoter region contained 353 bp from 659 to 907 nt in the plasmid with the sequence-

GAGGGCCTATTTCCCATGATTCCTTCATATTTGCATATACGATACAAGGCTGTTAG
AGAGATAATTGGAATTAATTTGACTGTAAACACAAAGATATTAGTACAAAATAC
GTGACGTAGAAAGTAATAATTTCTTGGGTAGTTTGCAGTTTTAAAATTATGTTTT
AAAATGGACTATCATATGCTTACCGTAACTTGAAAGTATTTCGATTTCTTGGCTT
TATATATCTTGTGGAAAGGACGAAACAC, followed by the BBsI site with 18 bp from 907 to 924 nt with the sequence CGGGTCTTCGAGAAGACC. From 925 to 1007 nt, the chimeric nucleotide sequence was present which contained 83 bp with the sequence-

TGTTTTAGAGCTAGAAATAGCAAGTTAAAATAAGGCTAGTCCGTTATCAACTTG
AAAAAGTGGCACCGAGTCGGTGCTTTTTT.

4.3 Cells Transfection

The wells A1 and A2 of the 12-well plate, represented in Figure 3a, showed the presence of GFP through the emission of green color when a fluorescent microscope was used to visualize the HEK293 cells. The presence of GFP in the cells indicates that the plasmids (pGFP) containing GFP were transfected into the cells using the Lipofectamine delivery method. Likewise, Figure 3b showed the growing cells in wells A3 and B1 that were transfected with plasmids containing gRNA, and plasmids containing dCas9-KRAB.

The successful transfection of plasmids in the positive control wells represented in Figure 3a indicates that the cultured cells had a viable transfection rate.

Cells with GFP

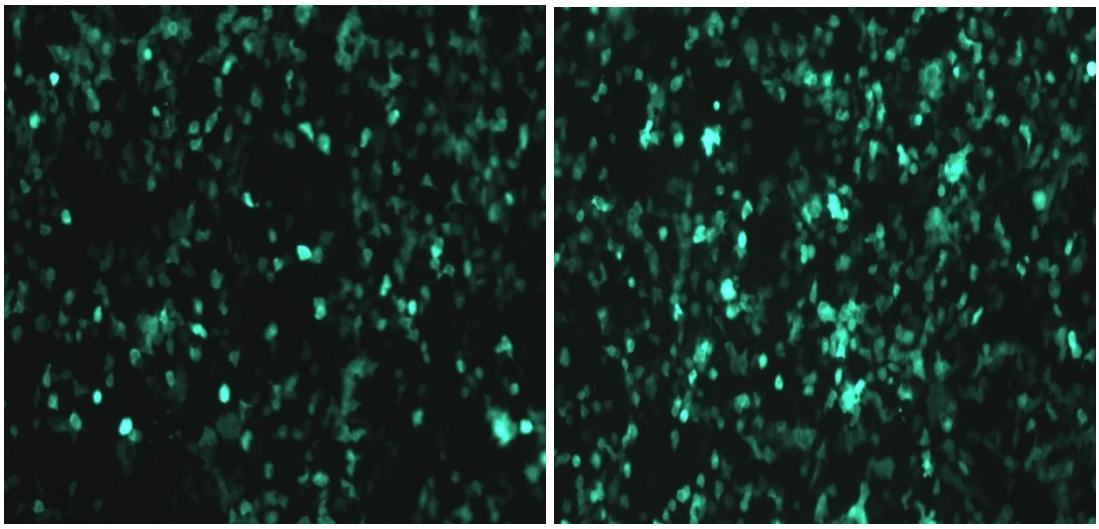

Figure 3a: Fluorescence Microscopy images of the HEK293 cells transfected with plasmids (pGFP) containing green fluorescent protein.

Cells with dCas9-KRAB and expression plasmids

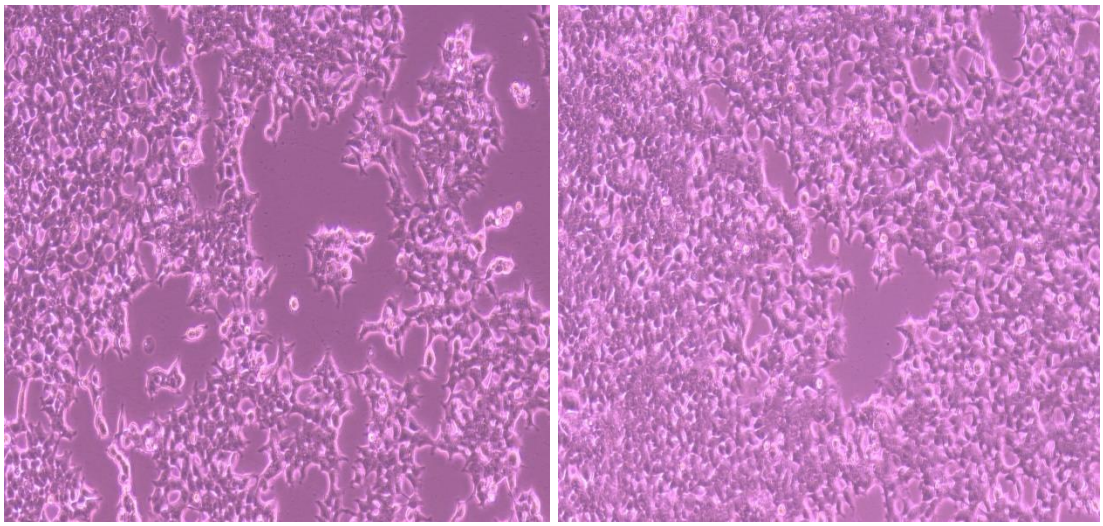

Figure 3b: Microscopy images of the HEK293 cells transfected with dCas9-KRAB-plasmid and expression plasmid vectors with gRNAs.

5. Discussion

In Figure 1, the presence of single bands in wells 3 and 4 indicate that plasmid vectors indicate that one restriction enzyme was used to make a single cut in the plasmid vector. With a single cut made in the plasmid, the plasmid retained its original size (~3.2 kb). Had there been more than one cut, two or more bands with the respective base-pairs would have appeared on the gel. The slow rate of migration shown by the bands in an electric field on gel electrophoresis indicates that the plasmid DNAs were not super-coiled because a super-coiled or an uncut plasmid DNA would have traveled down the gel towards the positive end at a higher rate.

The data obtained in Figure 2(b) shows a missing nucleotide "T" in the U6 promoter sequence at 706^{th} nucleotide in the plasmid backbone. However, the presence of the forward guide RNA insert in the BbsI restriction site indicates that the potential mismatch/noise was not significant in cloning the gRNA inserts into the expression plasmids. Similarly, the presence of all the forward gRNAs in their respective expression plasmids illustrated in Figures 2a-2e indicates the efficient digestion of plasmid, phosphorylation of oligos, and ligation of inserts into the expression vector.

The presence of Green Fluorescence Protein in Figure 3(a) confirms a successful transfection of plasmids into the HEK293 cells. Since the GFP was transfected into the cells in the form of genes present in a plasmid vector, it indicates that the genes for GFP were able to code for the respective protein in the cells. This serves as a positive control for the other transfected cells present in the 12-well plate. Image 3(b) indicated that the cells were viably cultured and passaged, however the expression of the target genes in the cells through RNA extraction was not confirmed.

CRISPRi has many advantages when compared to the traditional methods of gene repression like RNAi, TALEN/ ZF, and miRNA sponges. One of the advantages of CRISPRi over the other most widely used RNAi approach is that there is a very minimal off-target effect with CRISPRi. CRISPRi complexes that are situated near the TSS work towards inhibiting transcription, and because of a narrow binding region CRISPRi complex around the TSS, the sequence space is shortened, where the bindings could increase off-target activity. Also, because CRISPRi is already very sensitive to the sgRNA and target DNA mismatches, the off-target effect is not significant enough to affect the transcription in the genes (Gilbert et al., 2013)**,** (Kuscu et al., 2014), (Wu et al., 2014). CRISPRi can also be used to target the non-coding RNAs including miRNAs, lncRNAs, and the redundancy of miRNAs can be potentially targeted together. (Gilbert et al., 2013), (La Russa & Qi, 2015).

The activation and regulation of NF-κB are associated with genes like CAV1 and NFKBIZ. The upregulated expression of NF-κB, CAV1, and NFKBIZ negatively affected wound healing. While it remains vague whether the upregulation of NF-κB directly up-regulates the expression of CAV1 and NFKBIZ, they all affect wound-healing and are interconnected through other protein attachments and pathways in the wound-healing physiological process. The upregulation of TNF-α, TGF-β, AGE, RAGE, ROS, and dysregulation in VEGF, PDGF, and ET-1, are linked with the over-expression of NF-κB. They affect inflammatory responses, ECM deposition, and other physiological processes that are crucial in wound healing. (Collins & Cybulsky, 2001)**,** (Rask-Madsen & King, 2010)**,** (Takematsu et al., 2020)**,** (Jozic et al., 2019), (Bitar et al., 2013).

6. Conclusion

The Sanger sequencing results indicate that the forward guide RNA sequences were successfully inserted in the plasmid backbone at the BbsI restriction sites after the plasmid vector was digested and confirmed through an agarose gel electrophoresis. Likewise, the presence of GFP protein in the positive control indicated that the plasmids with the GFP gene were transfected and transcribed into the cultured HEK293 cells. This indicates that the extracted RNA from the transfected cells could potentially have an expressed dCas9-KRAB and gRNA complex for a repressed expression of target genes.

7. Future Directions

Using pre-designed forward and reverse primers for qPCR, the mRNA expression for NF-κB would be assessed through the RNA extracted from the transfected cells. The use of dCas9-KRAB indicates that a downregulated gene expression of NF-κB is to be expected. Downregulated RNA expression would indicate a successful CRISPRi approach using dcas9-KRAB. Since NF-κB is linked with many pathways and proteins that affect wound healing, successful in-vitro gene repression through dCas9-KRAB could be optimized and designed for potential in vivo studies. The plasmid vectors with the cloned gRNAs for NFKBIZ and Cav1 could be transfected with a similar approach as mentioned in this study. The relationship between NF-κB, NFKBIZ and Cav1 can be explored, and their collective roles in wound healing can be studied using a multiplexed genome engineering approach, by introducing a stabilizer tertiary RNA in the CRISPR/Cas complex (Campa et al., 2019).

8. Acknowledgement

I would like to express my sincere gratitude to Dr. Christopher Nelson for his continuous guidance and mentorship in my Honors research thesis project and throughout my undergraduate career. I would also like to thank Harumi Padmaswari for teaching me valuable lab techniques for my research project, and Daniel Maxenberger for helping me in my project. I am highly obliged to the Biomedical Engineering Department at the University of Arkansas for providing me with the opportunities to learn, connect and grow as a biomedical engineer.

References

Addgene. (2021). *Addgene's Crispr e-book* (3rd ed.).

Bitar, M. S., Abdel-Halim, S. M., & Al-Mulla, F. (2013). Caveolin-1/PTRF upregulation constitutes a mechanism for mediating p53-induced cellular senescence: implications for evidence-based therapy of delayed wound healing in diabetes.*American Journal of Physiology-Endocrinology and Metabolism*, *305*(8). https://doi.org/10.1152/ajpendo.00189.2013

Campa, C. C., Weisbach, N. R., Santinha, A. J., Incarnato, D., & Platt, R. J. (2019). Multiplexed genome engineering by Cas12a and CRISPR arrays encoded on single transcripts. *Nature Methods*, *16*(9), 887–893. https://doi.org/10.1038/s41592-019-0508-6

Cardarelli, F., Digiacomo, L., Marchini, C., Amici, A., Salomone, F., Fiume, G., … Caracciolo, G. (2016). The intracellular trafficking mechanism of Lipofectamine-based transfection reagents and its implication for gene delivery. *Scientific Reports*, *6*(1). https://doi.org/10.1038/srep25879

Carter, M., & Shieh, J. (2015). Gene Delivery Strategies. *Guide to Research Techniques in Neuroscience*, 239–252. https://doi.org/10.1016/b978-0-12-800511-8.00011-3

Collins, T., & Cybulsky, M. I. (2001). NF-κB: pivotal mediator or innocent bystander in atherogenesis? *Journal of Clinical Investigation*, *107*(3), 255–264. https://doi.org/10.1172/jci10373

CRISPR RGEN Tools. (n.d.). http://www.rgenome.net/

Doudna, J. A., & Charpentier, E. (2014). The new frontier of genome engineering with CRISPR-Cas9. *Science*, *346*(6213), 1258096. https://doi.org/10.1126/science.1258096

Gilbert, L. A., Larson, M. H., Morsut, L., Liu, Z., Brar, G. A., Torres, S. E., … Qi, L. S. (2013). CRISPR-Mediated Modular RNA-Guided Regulation of Transcription in Eukaryotes. *Cell*, *154*(2), 442–451. https://doi.org/10.1016/j.cell.2013.06.044

Inc., O. G. T. (n.d.). *qPCR Tools*. OriGene Technologies Inc. https://www.origene.com/products/gene-expression/qpcr.

Jinek, M., Chylinski, K., Fonfara, I., Hauer, M., Doudna, J. A., & Charpentier, E. (2012). A Programmable Dual-RNA-Guided DNA Endonuclease in Adaptive Bacterial Immunity. *Science*, *337*(6096), 816–821. https://doi.org/10.1126/science.1225829

Johnson, B. Z., Stevenson, A. W., Prêle, C. M., Fear, M. W., & Wood, F. M. (2020). The Role of IL-6 in Skin Fibrosis and Cutaneous Wound Healing. *Biomedicines*, *8*(5), 101. https://doi.org/10.3390/biomedicines8050101

Jozic, I., Sawaya, A. P., Pastar, I., Head, C. R., Wong, L. L., Glinos, G. D., … Tomic-Canic, M. (2019). Pharmacological and Genetic Inhibition of Caveolin-1 Promotes Epithelialization and Wound Closure. *Molecular Therapy*, *27*(11), 1992–2004. https://doi.org/10.1016/j.ymthe.2019.07.016

Khanna, S., Biswas, S., Shang, Y., Collard, E., Azad, A., Kauh, C., … Roy, S. (2010). Macrophage Dysfunction Impairs Resolution of Inflammation in the Wounds of

Diabetic Mice. *PLoS ONE*, *5*(3). https://doi.org/10.1371/journal.pone.0009539

Kitada, M., Zhang, Z., Mima, A., & King, G. L. (2010). Molecular mechanisms of diabetic vascular complications. *Journal of Diabetes Investigation*, *1*(3), 77–89. https://doi.org/10.1111/j.2040-1124.2010.00018.x

Kuscu, C., Arslan, S., Singh, R., Thorpe, J., & Adli, M. (2014). Genome-wide analysis reveals characteristics of off-target sites bound by the Cas9 endonuclease. *Nature Biotechnology*, *32*(7), 677–683. https://doi.org/10.1038/nbt.2916

La Russa, M. F., & Qi, L. S. (2015). The New State of the Art: Cas9 for Gene Activation and Repression. *Molecular and Cellular Biology*, *35*(22), 3800–3809. https://doi.org/10.1128/mcb.00512-15

Lipofectamine™ 3000 Reagent USER GUIDE. Document Connect. (n.d.). https://www.thermofisher.com/document-connect/document-connect.html?url=https%3A%2F%2Fassets.thermofisher.com%2FTFS-Assets%2FLSG%2Fmanuals%2Flipofectamine3000_protocol.pdf&title=TGlwb2ZlY3RhbWluZSAzMDAwIFJlYWdlbnQgUHJvdG9jb2wgKEVuZ2xpc2gp.

LV, X., LV, G.-H., DAI, G.-Y., SUN, H.-M., & XU, H.-Q. (2016). Food-advanced glycation end products aggravate the diabetic vascular complications via modulating the AGEs/RAGE pathway. *Chinese Journal of Natural Medicines*, *14*(11), 844–855. https://doi.org/10.1016/s1875-5364(16)30101-7

Molecular Cloning Techniques. Addgene. (n.d.). http://www.addgene.org/mol-bio-reference/cloning/.

Mohr, S. E., Hu, Y., Ewen-Campen, B., Housden, B. E., Viswanatha, R., & Perrimon, N. (2016). CRISPR guide RNA design for research applications. *The FEBS Journal*, *283*(17), 3232–3238. https://doi.org/10.1111/febs.13777

Ohnuma, K., Yamochi, T., Uchiyama, M., Nishibashi, K., Iwata, S., Hosono, O., … Morimoto, C. (2005). CD26 Mediates Dissociation of Tollip and IRAK-1 from Caveolin-1 and Induces Upregulation of CD86 on Antigen-Presenting Cells. *Molecular and Cellular Biology*, *25*(17), 7743–7757. https://doi.org/10.1128/mcb.25.17.7743-7757.2005

Qiagen. (n.d.). *RNeasy Mini Handbook - (EN)*. QIAGEN. https://www.qiagen.com/us/resources/resourcedetail?id=14e7cf6e-521a-4cf7-8cbc-bf9f6fa33e24&lang=en.

QIAprep Spin Miniprep Kit. QIAprep Spin Miniprep Kit - QIAGEN Online Shop. (n.d.). https://www.qiagen.com/us/products/discovery-and-translational-research/dna-rna-purification/dna-purification/plasmid-dna/qiaprep-spin-miniprep-kit/#orderinginformation.

Rask-Madsen, C., & King, G. L. (2010). Kidney complications: Factors that protect the diabetic vasculature. *Nature Medicine*, *16*(1), 40–41. https://doi.org/10.1038/nm0110-40

Sanger Sequencing at Eurofins Genomics. (n.d.). https://eurofinsgenomics.eu/en/custom-dna-sequencing/eurofins-services.

Schindele, P., Wolter, F., & Puchta, H. (2020). CRISPR Guide RNA Design Guidelines for Efficient Genome Editing. Methods in Molecular Biology, 331–342. https://doi.org/10.1007/978-1-0716-0712-1_19

Takematsu, E., Spencer, A., Auster, J., Chen, P.-C., Graham, A., Martin, P., & Baker, A. B. (2020). Genome wide analysis of gene expression changes in skin from patients with type 2 diabetes. *PLOS ONE*, *15*(2). https://doi.org/10.1371/journal.pone.0225267

Tobon-Velasco, J., Cuevas, E., & Torres-Ramos, M. (2014). Receptor for AGEs (RAGE) as Mediator of NF-kB Pathway Activation in Neuroinflammation and Oxidative Stress. *CNS & Neurological Disorders - Drug Targets*, *13*(9), 1615–1626. https://doi.org/10.2174/1871527313666140806144831

Trinh, D. V., Zhu, N., Farhang, G., Kim, B. J., & Huxford, T. (2008). The Nuclear IκB Protein IκBζ Specifically Binds NF-κB p50 Homodimers and Forms a Ternary Complex on κB DNA. *Journal of Molecular Biology*, *379*(1), 122–135. https://doi.org/10.1016/j.jmb.2008.03.060

U.S. National Library of Medicine. (n.d.). *BLAST: Basic Local Alignment Search Tool*. National Center for Biotechnology Information. https://blast.ncbi.nlm.nih.gov/Blast.cgi.

U.S. National Library of Medicine. (n.d.). *Primer designing tool*. National Center for Biotechnology Information. https://www.ncbi.nlm.nih.gov/tools/primer-blast/

UCSC Genome Browser Home. (n.d.). https://genome.ucsc.edu/.

Wu, X., Scott, D. A., Kriz, A. J., Chiu, A. C., Hsu, P. D., Dadon, D. B., … Sharp, P. A. (2014). Genome-wide binding of the CRISPR endonuclease Cas9 in mammalian cells. *Nature Biotechnology*, *32*(7), 670–676. https://doi.org/10.1038/nbt.288